Low doses of the neonicotinoid insecticide imidacloprid induce ROS triggering neurological and metabolic impairments in *Drosophila*

Felipe Martelli[a,1], Zuo Zhongyuan[b], Julia Wang[b], Ching-On Wong[c], Nicholas E. Karagas[d], Ute Roessner[a], Thusitha Rupasinghe[a,2], Kartik Venkatachalam[d], Trent Perry[a], Hugo J. Bellen[b,e,f,3], and Philip Batterham[a,3,4]

[a]School of BioSciences, The University of Melbourne, Parkville, VIC, 3052, Australia; [b]Department of Molecular and Human Genetics, Baylor College of Medicine, Houston, TX 77030; [c]Department of Biological Sciences, Rutgers University, Newark, NJ 07102; [d]Department of Integrative Biology and Pharmacology, McGovern Medical School at the University of Texas Health Sciences Center, Houston, TX 77030; [e]Neurological Research Institute, Texas Children's Hospital, Houston, TX 77030; and [f]Howard Hughes Medical Institute, Baylor College of Medicine, Houston, TX 77030

Edited by John G. Hildebrand, University of Arizona, Tucson, AZ, and approved August 27, 2020 (received for review June 8, 2020)

Declining insect population sizes are provoking grave concern around the world as insects play essential roles in food production and ecosystems. Environmental contamination by intense insecticide usage is consistently proposed as a significant contributor, among other threats. Many studies have demonstrated impacts of low doses of insecticides on insect behavior, but have not elucidated links to insecticidal activity at the molecular and cellular levels. Here, the histological, physiological, and behavioral impacts of imidacloprid are investigated in *Drosophila melanogaster*, an experimental organism exposed to insecticides in the field. We show that oxidative stress is a key factor in the mode of action of this insecticide at low doses. Imidacloprid produces an enduring flux of Ca^{2+} into neurons and a rapid increase in levels of reactive oxygen species (ROS) in the larval brain. It affects mitochondrial function, energy levels, the lipid environment, and transcriptomic profiles. Use of RNAi to induce ROS production in the brain recapitulates insecticide-induced phenotypes in the metabolic tissues, indicating that a signal from neurons is responsible. Chronic low level exposures in adults lead to mitochondrial dysfunction, severe damage to glial cells, and impaired vision. The potent antioxidant, *N*-acetylcysteine amide (NACA), reduces the severity of a number of the imidacloprid-induced phenotypes, indicating a causal role for oxidative stress. Given that other insecticides are known to generate oxidative stress, this research has wider implications. The systemic impairment of several key biological functions, including vision, reported here would reduce the resilience of insects facing other environmental challenges.

imidacloprid | lipid dysregulation | neurodegeneration | oxidative stress | vision loss

Insects make up a significant proportion of global biodiversity, with estimates of the number of extant species ranging up to 5.5 million (1). Insects provide many essential services, including pollination, pest control, nutrient recycling, and food resources for other animals (2). A limited number of insect species are pests. A recent metaanalysis reported an average decline of terrestrial insect abundance of ∼9% per decade since 1925 (3). While this is a lower rate of decline than reported in earlier studies (4), it suggests that many insect species are under serious threat. Insecticide exposure is consistently proposed to be one of the significant contributing factors (2, 4). Insects that share habitats with pests may be exposed to lethal insecticide concentrations (5, 6), but most nonpest species are probably exposed to doses that kill slowly, if at all. Studies have shown evidence of the impact of such doses on the behavior of insects (7, 8), but the broader biological effects of exposure have not been systematically investigated. Insecticides act by perturbing the function of the protein targets to which they bind. The molecular mechanisms by which this triggers downstream effects in insects that survive insecticide exposure have not been identified. Exposure to a range of insecticides differing in their chemical structure has been shown to increase the levels of reactive oxygen species (ROS) (9–11). Links between low dose exposures, ROS, and perturbations in behavior have been proposed, but not examined in detail (12). Investigation of these links may help us understand the relationship between insecticide use and the decline in insect populations.

The neonicotinoid insecticide imidacloprid has been subjected to intense scrutiny. This has been due to the publication of evidence that adverse impacts on behavior may contribute to colony collapse disorder in honey bees (13), an organism in which imidacloprid is known to create some level of oxidative stress (14). Although banned from use in agricultural settings by the European Union, imidacloprid remains one of the top selling insecticides in the world (15). Imidacloprid is a systemic insecticide which, along with its high water solubility, creates the potential for the exposure of insects consuming pollen, nectar, plant

Significance

Intense insecticide usage is suggested to be a significant contributor to the observed decline of insect populations around the world. Beneficial insects play essential roles in food production and ecosystem health. It is therefore vital to understand the mechanisms by which low doses of insecticide impact insect biology in order to understand and assess the threat posed. We investigated the impacts of the neonicotinoid insecticide imidacloprid on *Drosophila*. The binding of the insecticide to receptors in the brain triggers oxidative stress, reduces energy levels, and induces neurodegeneration as well as vision loss. As the receptors targeted by imidacloprid are conserved among insects, and other insecticides have also been shown to cause oxidative stress, these findings have wider significance.

Author contributions: F.M., C.-O.W., U.R., K.V., T.P., H.J.B., and P.B. designed research; F.M., Z.Z., J.W., C.-O.W., N.E.K., and T.R. performed research; T.P. contributed new reagents/analytic tools; F.M., Z.Z., and T.R. analyzed data; and F.M., U.R., K.V., T.P., H.J.B., and P.B. wrote the paper.

The authors declare no competing interest.

This article is a PNAS Direct Submission.

This open access article is distributed under Creative Commons Attribution-NonCommercial-NoDerivatives License 4.0 (CC BY-NC-ND).

[1]Present address: School of Biological Sciences, Monash University, Clayton, VIC, 3800, Australia.

[2]Present address: SCIEX, Life Science Research (Lipidomics), VIC, 3170, Australia.

[3]H.J.B. and P.B. contributed equally to this work.

[4]To whom correspondence may be addressed. Email: p.batterham@unimelb.edu.au.

This article contains supporting information online at https://www.pnas.org/lookup/suppl/doi:10.1073/pnas.2011828117/-/DCSupplemental.

Downloaded by guest on September 30, 2020

exudates, and tissues and for aquatic insects dwelling in runoff water (16). Imidacloprid targets nicotinic acetylcholine receptors (nAChRs) in the central nervous system (17), that are conserved among insects (18). nAChRs are pentameric ligand-gated cation channels that, once activated, lead to Ca^{2+}, Na^{+}, or K^{+} flux into neurons, regulating a myriad of responses (18). The binding of the natural ligand, acetylcholine (ACh), to the extracellular domain of nAChRs leads to channel opening, while hydrolysis of ACh by acetylcholinesterase leads to the channel closing. Imidacloprid occupies a binding site that overlaps with the ACh binding site. In contrast with ACh, imidacloprid is not hydrolyzed, so binding leads to sustained channel opening (19). Hence, acute exposure to high doses of this insecticide causes neuronal excitotoxicity and rapid death (20). There are 10 nAChR subunit genes in *Drosophila melanogaster*. Imidacloprid has been shown to target the α1 and β2 subunits (17). *Drosophila* loss-of-function mutants for these genes are only moderately resistant (17), indicating that imidacloprid may target nAChR subtypes that contain additional subunits. Recent heterologous expression studies indicate that the α1, α2, β1, and β2 subunits contribute to nAChRs targeted by imidacloprid (21). The molecular and cellular events downstream of imidacloprid binding to an nAChR have not been described. Here we examine systemic impacts on metabolism and brain function caused by low level exposures to this insecticide in *D. melanogaster* larvae and adults. We show that oxidative stress, precipitated by the binding of imidacloprid to nAChRs, is a key factor in its mode of action at low doses, triggering a cascade of damage resulting in reduced energy levels, neurodegeneration, and blindness, which should increase insect susceptibility to other environmental stresses.

Results

Imidacloprid Induces Ca^{2+} Flux into Neurons, Oxidative Stress, and Mitochondrial Dysfunction. In the field, imidacloprid is variously sprayed at concentrations of 50 to 100 ppm (parts per million) or applied to soil for uptake into plant tissues at 350 to 2,800 ppm (22). To initiate our studies, we identified an acute dose (2.5 ppm) that reduced the level of *Drosophila* third instar larval movement by 50% over a 2-h exposure period (Fig. 1*A*). This dose did not have a significant impact on survival when exposed larvae were placed back onto insecticide-free food medium and allowed to develop to adulthood (Fig. 1*B*). The impact of imidacloprid (2.5 ppm) on Ca^{2+} flux into neurons was investigated as Ca^{2+} can increase levels of ROS via a variety of mechanisms, such as the activation of nitric oxide synthase (NOS) yielding nitric oxide, which inhibits complex IV and Ca^{2+} overloading of the mitochondrial matrix (23). This dose (2.5 ppm) elicited a low, enduring Ca^{2+} elevation in nAChR-expressing neurons when assessed using the GCaMP5G:tdTomato cytosolic [Ca^{2+}] sensor (Fig. 1 *C* and *D*). After a 5-min treatment with the insecticide, neurons were exposed to carbachol, an analog of ACh. Imidacloprid-treated cells showed a 2.2-fold reduction in cholinergic response, presumably because imidacloprid molecules compete with carbachol for nAChR binding. In contrast, total endoplasmic reticulum (ER) Ca^{2+} mobilized by application of the ER pump inhibitor, thapsigargin, was not significantly different in control and imidacloprid-treated cells (Fig. 1 *C* and *D*), indicating that ER Ca^{2+} content remained unaltered. Furthermore, a 1-h exposure to 2.5 ppm imidacloprid increased the levels of superoxide in the larval brain (Fig. 1 *E* and *F*). The same effect was observed in the midgut, but required a 2-h exposure. Thus, an increase in the levels of ROS in the midgut is preceded by an increase in the brain (Fig. 1 *E* and *F*). No increases in superoxide levels were detected in any other tissues. After a 2-h exposure, the activity of aconitase, a mitochondrial enzyme that is highly sensitive to elevated levels of ROS (24), was reduced by 30% and ATP levels were decreased by 20% in whole animals (Fig. 1*G*). These data suggest mitochondrial dysfunction so we examined mitochondrial turnover using the MitoTimer line (25). Increased levels of both healthy and unhealthy mitochondria were observed in brain and in the anterior portion of the alimentary canal—the proventriculus (*SI Appendix*, Fig. S1). In summary, 2.5 ppm imidacloprid causes a sustained Ca^{2+} flux into neurons, an increase in mitochondrial ROS, and a decrease in ATP production.

Increasing ROS in the Brain Causes Perturbations of the Lipid Environment in Metabolic Tissues. High levels of oxidative stress associated with a loss of mitochondrial aconitase activity in neurons, have been shown to induce the accumulation of lipid droplets (LDs) in glial cells (26, 27). Storage of lipids in LDs renders them less susceptible to peroxidation (28). As ROS was detected in the brain prior to other tissues, we tested whether ROS generated by mitochondrial dysfunction in neurons might lead to the accumulation of LDs in other tissues. The *elav* neuronal driver was used to knock down the expression of two genes encoding proteins required for mitochondrial electron transport, *ND42* (NADH dehydrogenase [ubiquinone] 1 alpha subcomplex subunit 10) and *Marf* (mitochondrial assembly regulatory factor) using RNAi. Knockdown of these genes has been previously shown to cause elevated levels of ROS and the accumulation of LDs in glial cells in the retinas of adult flies (26). Although limited to neurons, knockdown of *ND42* and *Marf* increased the area occupied by LDs in fat body by an average of 49.7% and 54.7%, respectively. In contrast, an average reduction of 72.3% and 74% in LD numbers in Malpighian tubules was observed for *ND42* and *Marf* knockdown, respectively (Fig. 2 *A* and *B*). Even though the overall response in fat bodies was a consistent increase in the area occupied by LDs, we observed a significant reduction in the number of large LDs and an increase in small LDs (*SI Appendix*, Fig. S2). Hence, oxidative stress initiated in neurons causes an accumulation of LDs of altered size in fat bodies.

Having observed that the generation of elevated levels of ROS in neurons is associated with an increase in LD density and numbers in fat body and reduction in Malpighian tubules, we tested whether imidacloprid exposure could trigger the same effect (Fig. 3). Exposure to 2.5 ppm imidacloprid for 2 h elevated the area occupied by LDs in fat body by an average of 19% (Fig. 3 *A* and *B*), once again causing a reduction in the number of large LDs and an increase in the number of small LDs (*SI Appendix*, Fig. S3 *A* and *B*). In Malpighian tubules imidacloprid exposure caused an 95.5% mean reduction in LD numbers (Fig. 3 *C* and *D*). The recapitulation of the phenotypes observed with the knockdown of mitochondrial genes in neurons suggested that the impacts of imidacloprid on metabolic tissues is driven by ROS generated in the nervous system. To test this hypothesis, we examined whether treatment with an antioxidant could rescue the fat body phenotype. Pretreatment with an antioxidant, *N*-acetylcysteine amide (NACA) (29) rescued this phenotype (Fig. 3 *A* and *B* and *SI Appendix*, Fig. S3*A*) and significantly improved the movement of exposed larvae (*SI Appendix*, Fig. S4), showing that insecticide-induced oxidative stress is a trigger for these impacts. With imidacloprid exposure, under the same conditions, we also detected a reduction in lipid stores in midguts and levels of lipids in the hemolymph (*SI Appendix*, Fig. S3 *B* and *C*).

Imidacloprid Triggers Significant Changes in the Lipidome. To address the major changes observed in the lipid environment of larvae exposed to 2.5 ppm imidacloprid for 2 h, we performed a lipidomic analysis on whole larvae. While this analysis lacked the capacity to detect differences in specific tissues, it detected a more systemic response to imidacloprid exposure and identified the lipid classes affected (Fig. 4 *A*–*C* and *SI Appendix*, Table S1).

Downloaded by guest on September 30, 2020

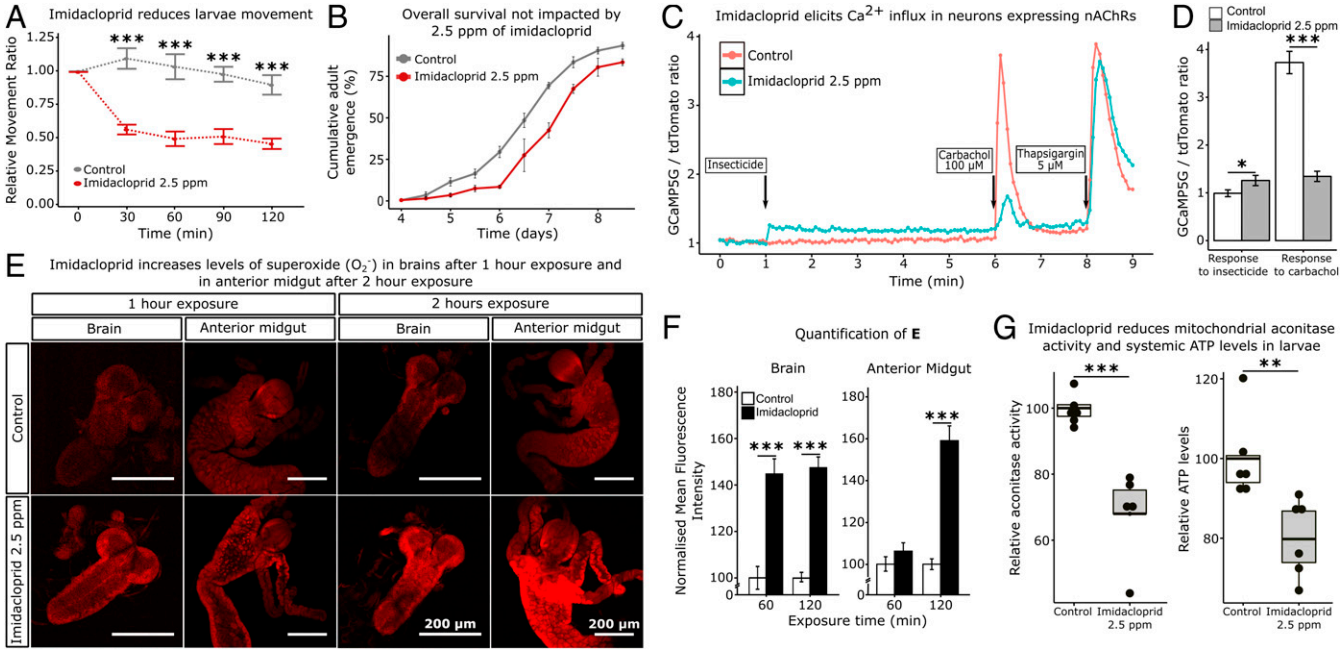

Fig. 1. Imidacloprid impacts are initiated in the brain. (*A*) Dose–response to insecticide by an assay of larval movement over time, expressed in terms of relative movement ratio (RMR); $n = 100$ larvae/treatment). (*B*) Cumulative adult emergence (%) following larval exposure to 2.5 ppm imidacloprid for 2 h ($n = 100$ larvae/treatment). (*C*) Ca^{2+} influx measured by GCaMP in neuronal cells expressing nAChR. Measurement is expressed in terms of GCaMP5G signal divided by tdTomato constitutive expression. After 1 min the imidacloprid group was exposed to a 2.5 ppm of the insecticide. At 6 min and 8 min the imidacloprid and control groups were exposed to 100 µM carbachol and 5 µM thapsigargin, respectively. Each point represents the average of at least 50 cells. (*D*) Ca^{2+} influx, peak responses to imidacloprid and carbachol. (*E*) Superoxide levels in the brain and anterior midgut of larvae exposed to 2.5 ppm imidacloprid for either 1 h or 2 h. Tissue stained with DHE. Images obtained in Leica SP5 laser scanning confocal microscope, 200× magnification. (*F*) Normalized mean fluorescence intensity ($n = 15$ larvae/treatment; 3 sections/larva). (*G*) Relative mitochondrial aconitase activity ($n = 25$ larvae/replicate; 6 replicates/treatment) and relative ATP levels ($n = 20$ larvae/replicate; 6 replicates/treatment) in whole larvae after exposure to 2.5 ppm imidacloprid for 2 h. Error bars in *A*, *B*, *D*, and *F* represent mean ± SEM *t* test; $*P < 0.05$; $**P < 0.01$; $***P < 0.001$. No significant difference found in *B* (Kolmogorov–Smirnov test; $P > 0.05$).

Multivariate analysis (Fig. 4*B*) indicates that even though only 34 out of 378 detected lipids were significantly impacted, the lipidomic profile of samples from exposed larvae cluster together and away from control samples. A significant portion of the observed impacts corresponds to a reduction in some phosphatidylcholine (PC) and phosphatidylethanolamine (PE) species in exposed larvae. In *Drosophila* larvae, ∼90% of membrane lipid is composed of glycerophospholipids; PE represents 65% of it, followed by PC (30). The reduction in overall PE levels is consistent with impaired membrane function. PE is an important determinant of membrane fluidity, regulating the lipid bilayer rigidity (31). PCs are also key regulators of LD dynamics (32). Along with observed alterations in some triacylglycerols (TAGs) (33), the major storage species of lipids, this may underpin the changes in the LDs in metabolic tissues. A significant increase in three oxidized phospholipid species was also observed (HPOT keto 34:2-PG-/16:0, HPOD keto 34:3-PG-/16:0, and M34:2-PE-/18:2) as well as a significant decrease in another (HOT 36:6-PC-/18:3). A large decrease (48.5%) in the total levels of the identified cardiolipins (Fig. 4*C*) was also observed. Cardiolipins are a class of lipids located in the inner mitochondrial membrane that anchor electron transport chain proteins. Reduction

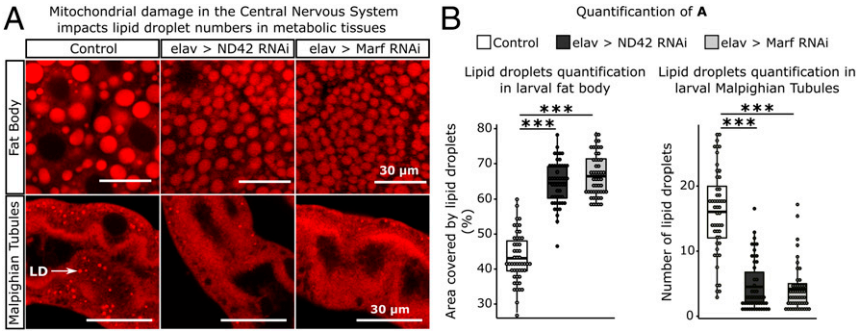

Fig. 2. Inducing ROS in the brain impacts the lipid environment of metabolic tissues. (*A*) Knockdown of genes encoding mitochondrial components, ND42 and Marf, in neurons caused the accumulation of LDs in larval fat body and a reduction of LD numbers in larval Malpighian tubules. White arrow indicates LD in Malpighian tubules. Tissues were stained with Nile Red and images obtained in a Leica SP8 laser scanning confocal microscope, 400× magnification. Images were analyzed using the software ImageJ. (*B*) Quantification of the area covered by LDs per section of 50 µm × 50 µm in larval fat body; and number of LDs per section of 30 µm × 30 µm in larval Malpighian tubules ($n = 10$ larvae/treatment; 5 sections/larva). *t* test; $***P < 0.001$.

Downloaded by guest on September 30, 2020

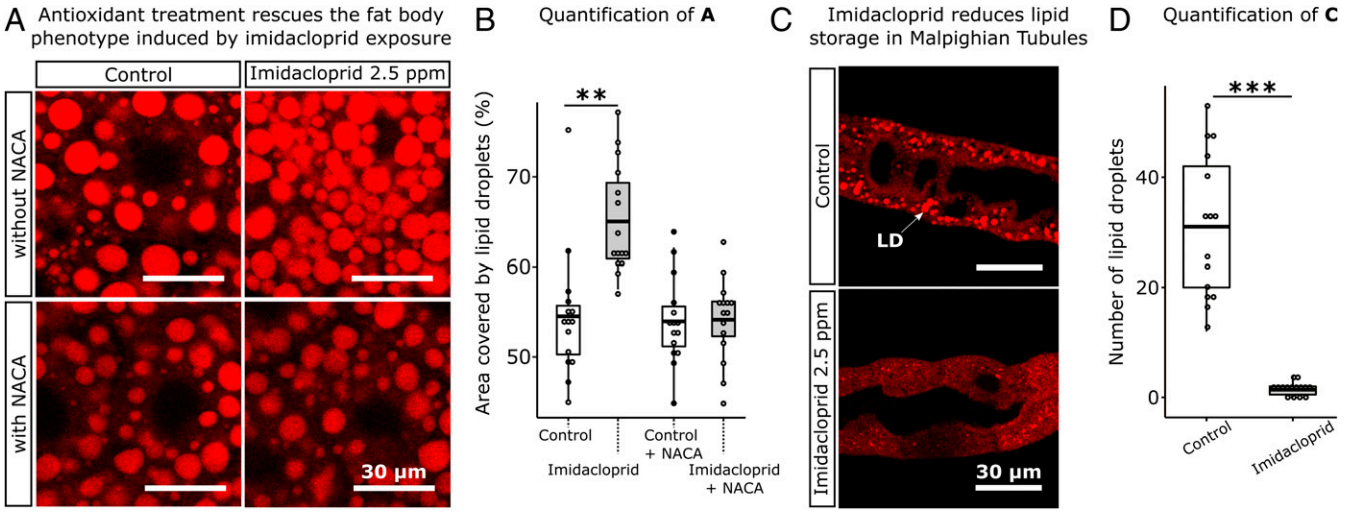

Fig. 3. Imidacloprid perturbs the lipid environment of metabolic tissues and antioxidant treatment rescues the fat body phenotype. (*A*) Larvae exposed to imidacloprid show a significant increase in the area occupied by LDs in fat body, whereas larvae pretreated with 75 µg/mL of antioxidant NACA for 5 h prior to imidacloprid exposure show no significant changes in the area occupied by LDs in fat body. (Scale bar: 30 µm.) (*B*) Percentage of area occupied by LDs in fat body sections of 50 µm × 50 µm ($n = 3$ larvae/treatment; 5 sections/larva). (*C*) Reduced number of LDs in Malpighian tubules of larvae exposed to imidacloprid. White arrow indicates a LD. (*D*) Number of LDs per section of 30 µm × 30 µm in larval Malpighian tubules section of 30 µm × 30 µm ($n = 3$ larvae/treatment; 5 sections/larva). Images obtained in a Leica SP5 laser scanning confocal microscope, 400× magnification. *t* test; $^{**}P < 0.01$; $^{***}P < 0.001$.

in cardiolipins levels is indicative of defects in electron transport complex I (34). Loss of complex I function is associated with increased ROS (35), which is in accordance with the observed reduction in mitochondrial aconitase activity, an enzyme that is extremely sensitive to high levels of ROS and the reduced ATP levels.

Imidacloprid Perturbs the Expression of Genes Related to Stress Response, Metabolism, Immunity, and Neurodegeneration. To investigate the impacts of imidacloprid (2.5 ppm for 2 h) on gene expression, a transcriptomic analysis of brains and fat bodies was conducted. The expression of 796 out of 9,640 transcripts was perturbed in brains (foldchange > |2|, adjusted [adj] *P* value <0.05),

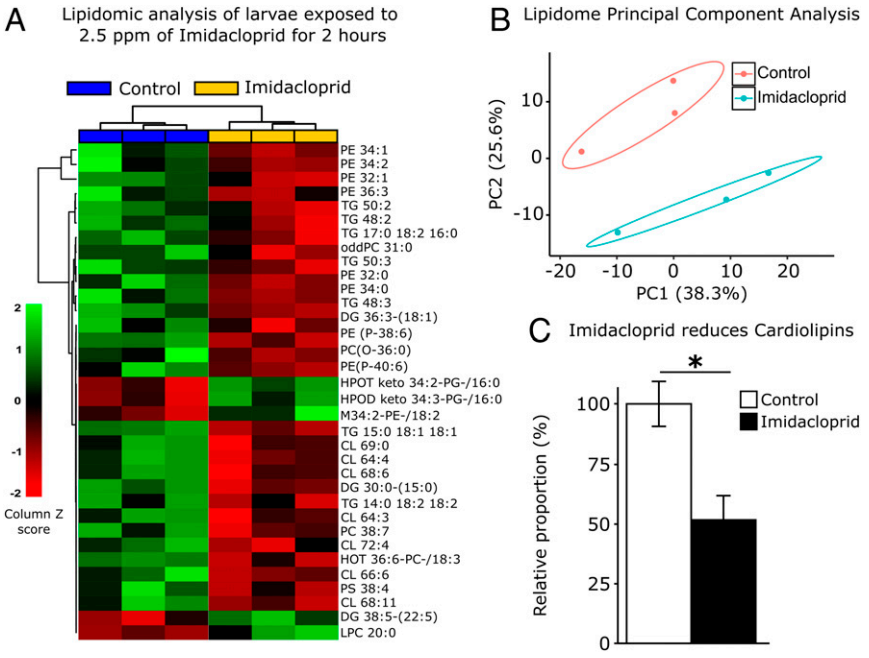

Fig. 4. Imidacloprid disturbs lipid profiles of exposed larvae. Lipidomic profile of larvae exposed to 2.5 ppm imidacloprid for 2 h ($n = 10$ larvae/replicate; 3 replicates/treatment). (*A*) A total of 34 lipid species out of 378 were significantly affected by insecticide treatment (one-way ANOVA, Turkey's honestly significant difference [HSD], $P < 0.05$). The column Z score is calculated subtracting from each value within a row the mean of the row and then dividing the resulting values by the SD of the row. The features are color coded by row, with red indicating low intensity and green indicating high intensity. (*B*) Principal component analysis of 378 lipid species. Each dot represents the lipidome data sum of each sample. First component explains 38.3% of variance and second component explains 25.6% of variance. (*C*) Relative proportion of cardiolipins in exposed animals versus control. Error bars represent mean ± SEM *t* test; $^{*}P < 0.05$.

Downloaded by guest on September 30, 2020

while in fat bodies 421 out of 9,564 transcripts were impacted (foldchange > |2|, adj *P* value <0.05) (Fig. 5). Gene ontology (GO) analysis and Kyoto Encyclopedia of Genes and Genomes (KEGG) pathway analysis suggested overall impacts on metabolism of xenobiotics by cytochrome P450s, oxidation-reduction process, metabolism of carbohydrates and amino acids, and immune response (Fig. 5). Analysis of individual genes in these functional groups was conducted. Genes involved in the regulation of the JNK (such as *bsk*, *Hep*, and *kay*) (36) and Cnc (such as *Maf-s* and *Keap1*) (37, 38) stress pathways were up-regulated in brains of exposed larvae (*SI Appendix*, Table S2).

Signatures of oxidative stress are observed in the brain under conditions of imidacloprid exposure. *Nitric oxide synthase* (*Nos*) expression levels increased 1.7-fold (*SI Appendix*, Table S2). Nitric oxide synthase is activated by Ca^{2+} to produce nitric oxide (NO), leading to oxidative stress in mitochondria (23). Consistent with this, the levels of several mitochondrial genes encoding complex I, III, and IV protein showed a subtle, but significant, up-regulation (*SI Appendix*, Table S2) (39). NADPH oxidase, encoded by *Nox* and *Duox*, catalyze the production of a superoxide free radical by transferring one electron to oxygen from NADPH (40). However, *Nox* levels were reduced by 2.8-fold and *Duox* levels were not impacted, suggesting that NADH oxidase is not likely to be involved. The antioxidant enzymes *Sod2*, responsible for the detoxifying superoxide radicals produced in mitochondria, was up-regulated, but *Catalase* which clears hydrogen peroxide in peroxisomes was down-regulated. Genes involved in the regulation of the JNK (such as *bsk*, *Hep*, and *kay*) (36) and Cnc (such as *Maf-s* and *Keap1*) pathways that respond to oxidative stress (37, 38) were up-regulated in brains of exposed larvae. In stark contrast, there is a striking lack of change of expression for almost all of these genes in the fat body. Some cytochrome P450 and GST enzymes play an important role in the detoxification of insecticides. Of the 86 P450 genes present in *Drosophila* (41), 15 had their expression perturbed by imidacloprid. In most cases this was a modest, though significant increase in expression in the brain (*SI Appendix*, Table S2). Two *Drosophila* P450s are known to metabolize imidacloprid, CYPG1 and CYP6G2 (42). The *Cyp6g2* gene is up-regulated in the brain; *Cyp6g1* is not. Among the 35 genes encoding GST enzymes in *Drosophila*, 20 showed altered expression in brain, fat body, or both (*SI Appendix*, Table S2). Six GSTs had increased expression in the brain and five showed a decrease, with these changes being small. For the fat body there was a more consistent trend with 9 of the 11 genes having a reduced level of expression.

Several proteins involved in lipid homeostasis, and induced by ROS, are up-regulated in exposed flies (*SI Appendix*, Table S2). These include the transcription factors SREBP and Mef2 that were up-regulated in the brain. SREBP is a central player in fatty acid synthesis. Mef2 promotes the expression of lipogenic and glycogenic enzymes and, upon infection, promotes the expression of antimicrobial peptides (43). In addition, several genes previously shown to be involved in the formation of LDs (27) are up-regulated in the brain. These include *Silnoon* and *outsiders* which encode monocarboxylate transporters and *Basigin* which encodes an accessory protein of Silnoon and Outsiders. These monocarboxylate transporters allow lactate from glial cells to be imported into neurons to provide the energy source for the synthesis of lipids. We also observed an up-regulation of lactate dehydrogenase (*ldh*) that is required to form pyruvate from lactate, an up-regulation of pyruvate dehydrogenases (*pdha* and *pdhb*) to produce acetyl-CoA, and citrate synthase (*kdn*) to converts acetyl-CoA into citrate, a substrate for lipogenesis. Hence, increased levels of acetyl-CoA combined with elevated levels of SREBP provide the neurons with the ability to increase

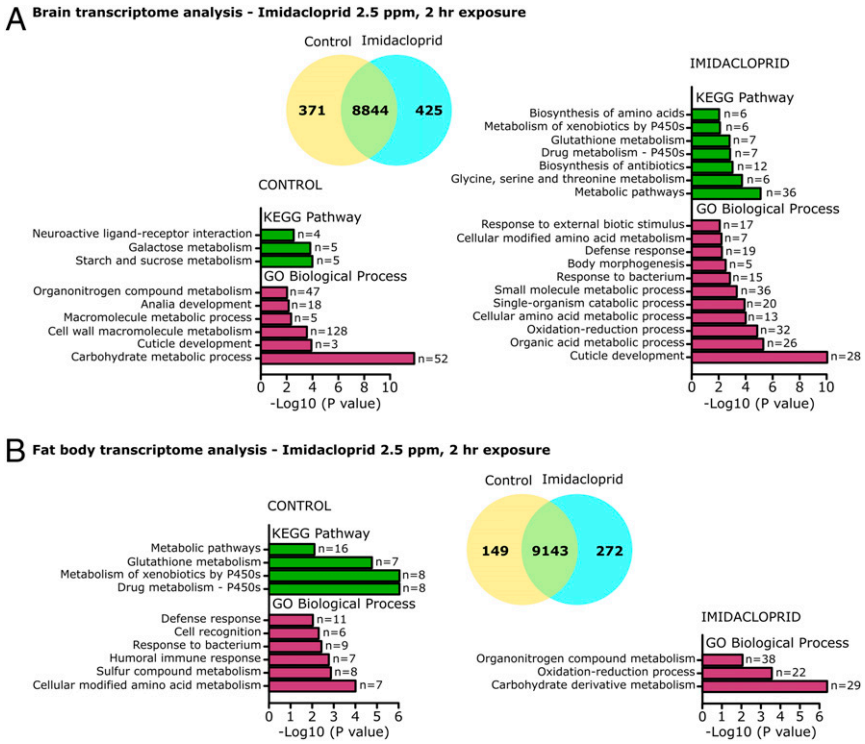

Fig. 5. Transcriptomic analysis of the brain and fat body of larvae acutely exposed to imidacloprid. Third instar larvae exposed to 2.5 ppm imidacloprid for 2 h ($n = 40$ larvae/sample; 3 samples/treatment). (*A*) Transcriptomic analysis of brains, 371 genes down-regulated, and 425 genes up-regulated in imidacloprid samples (foldchange > |2|, *P* adj < 0.05). (*B*) Transcriptomic analysis of fat body, 149 genes down-regulated, and 272 genes up-regulated in imidacloprid samples (foldchange > |2|, *P* adj < 0.05). KEGG and Gene Ontology analysis were performed in DAVID (Bioinformatics Resources 6.8), the modified Fisher exact *P* value was transformed using −log (10) scale. The "n" values in front of the bars indicate the number of genes associated to each KEGG Pathway or GO biological process in the dataset.

Downloaded by guest on September 30, 2020

lipid synthesis (26). These lipids are typically peroxidized and exported from neurons via ABCA transporters where they are captured by Glial Lazarillo (27).

The expression levels of the key genes for lipid biosynthesis, such as *mdy* and *Dgat2* (TAG synthesis), *ACC* (catalyses malonyl-CoA, the rate-limiting substrate for fatty acid synthesis), and *FASN1*, *FASN2*, and *FASN3* (fatty acid synthases), were not altered. In contrast, the expression of three genes (*LRP1*, *apolpp*, and *Apoltp*) that encode proteins involved in lipid transport between tissues via the hemolymph were up-regulated in brain and, in the case of *LRP1*, also in fat body (*SI Appendix*, Table S2). These data, in combination with the altered lipid levels in hemolymph, suggest that lipid synthesis is occurring in the fat body at normal levels and that the process responsible for the accumulation of lipids in this organ is lipid mobilization.

Many genes encoding subunits of serotonin, dopamine, muscarinic, and nicotinic acetylcholine, octopamine, GABA, and glutamate receptors were also affected by imidacloprid exposure (*SI Appendix*, Table S2). This included 9 of the 10 genes for nAChR subunits. In all cases there was a subtle but significant increase in the expression of these genes in the brain.

Finally, the transcriptomic analysis revealed the impact of imidacloprid exposures on several genes involved in immune response (*SI Appendix*, Table S2). Other studies have noted the adverse effects of insecticide exposure on the immune system of nontarget insects (44, 45), a process for which there is currently no clear mechanism. The immune response in *Drosophila* is mediated by the production of antimicrobial peptides (AMPs), which is regulated by two distinct pathways, Toll and immune deficiency (IMD) pathways, through the activation of transcription factors such as Relish and Dorsal (46). The genes encoding the AMPs are among those most affected by imidacloprid exposure. The AMP *Diptericin A* gene showed more than a 40-fold reduction in expression in the brain and more than a 200-fold reduction in fat body. AMP *Drosomycin-like 2* showed more than a 500-fold reduction in the brain. Several other components of innate immune response in *Drosophila* were also affected, including the factors Relish and Dorsal which showed increased expression in the brain (*SI Appendix*, Table S2). The increase in expression of *Relish* and *Dorsal* seems inconsistent with the down-regulation of AMPs. It suggests that other factors were involved in regulating the expression of the AMPs in exposed insects.

Chronic Exposures to Imidacloprid Cause Neurodegeneration and Vision Loss. To examine the effects of chronic exposure to imidacloprid in adult flies, we used a dose that causes 50% mortality within a 20- to 25-d period, 4 ppm (Fig. 6*A*). This dose has no significant impact on survival for the first 10 d and allows us to examine functional and morphological defects in the nervous system of adults a long time prior to inducing severe phenotypes. Importantly, the longevity of flies treated with imidacloprid was significantly rescued in the presence of NACA as the survival rate increased from 47 to 83% at day 25 (Fig. 6*A*). A similar observation was recently reported for the silk moth (47). To address the impact of imidacloprid on nervous system morphology and function, we assessed a suite of nervous system phenotypes. Transmission electron microscopy of the retina showed that exposure to 4 ppm imidacloprid for 20 d causes a massive vacuolization of the pigment cells/glia with a concomitant increase in the numbers of pigment granules and mitochondria in photoreceptors (PRs) (Fig. 6 *B*–*E*). The increased number of mitochondria, when combined with the observations related to MitoTimer in larvae, indicate that mitochondrial biogenesis is induced, likely to compensate for the cellular stress and mitochondrial damage induced by Ca^{2+} and/or ROS (48). Accordingly, a significant number of defective mitochondria were present in PR cells in the retinas of exposed flies (*SI Appendix*, Fig. S5). PRs are very sensitive to the loss of ATP production due to high energy consumption of the visual system (49).

To assess the effect of chronic exposures of imidacloprid on vision, we performed electroretinograms (ERGs) at regular intervals over a 20-d period. ERG recordings measure impulses induced by light. The on-transient is indicative of synaptic transmission between PR neurons and postsynaptic cells and the amplitude measures the phototransduction cascade (50). A reduction in the on-transient was observed starting at day 5 and a reduction in amplitude from day 10 onward (Fig. 7 *A*–*C*). These defects indicate that the flies gradually become severely visually impaired as both synaptic transmission and phototransduction are compromised (50). We also tested the flies using two different behavioral paradigms. Bang sensitivity is typically associated with defects in mitochondrial function (51) and assesses the propensity for seizures to occur. This assay measures the time it takes for flies to recover to a standing position following mechanical shock induced by vortexing. Significant differences between exposed flies and unexposed controls were first observed after 10 d, but these increased substantially after 20 d (Fig. 7*D*). Exposed flies also performed poorly in climbing assays. This phenotype is often linked to neurodegeneration (52) (Fig. 7*E*). Totals of 6%, 44%, and 68% of flies failed to climb after 1, 10, and 20 d of exposure, respectively. Again, the climbing ability was significantly less impacted in flies exposed to the same dose of imidacloprid, but concomitantly treated with NACA. Here failure ratios of 7%, 13%, and 31% for the respective time points of 1, 10, and 20 d were observed (Fig. 7*E*). Hence, elevated levels of ROS clearly play a role in the observed defects in adults.

Discussion

In this study we link the known mode of action of the neonicotinoid insecticide imidacloprid in activating nAChRs with a cascade of downstream effects—ROS generation, oxidative stress, mitochondrial dysfunction, energy loss, lipid mobilization, and neurodegeneration leading to blindness in the model *D. melanogaster*. Elevated levels of ROS creating oxidative stress in the nervous system can account for many of the downstream impacts. The significant amelioration of the accumulation of LDs in the fat body, impaired larval movement and adult climbing ability, and reduced adult longevity by the antioxidant NACA strongly supports this conclusion.

Neonicotinoids, like imidacloprid, act by binding to nAChRs, causing a constitutive flux of cations into neurons. The GCaMP assay conducted here showed that imidacloprid caused a low, but enduring, Ca^{2+} flux into neurons expressing nAChRs. Elevated intracellular levels of Ca^{2+} are known to increase the production of ROS, which causes oxidative stress and are associated with mitochondrial dysfunction (23). The transcriptomic data suggest that the increased level of superoxide in the larval brain observed with dihydroethidium (DHE) staining (Fig. 1 *E* and *F*) is not produced by elevated expression of NADPH oxidases (*Nox* and *Duox*), but is rather a byproduct of mitochondrial damage. This could be caused by the increased expression and activation of NOS or the direct impact of Ca^{2+} on mitochondrial membranes (23). Increased *Nos* expression was observed in the brain. That the levels of ROS being generated lead to oxidative stress is indicated by a reduction in mitochondrial aconitase activity, an increase in mitochondrial turnover, and depletion of ATP levels when larvae are exposed to 2.5 ppm imidacloprid for 2 h (Fig. 1*G* and *SI Appendix*, Fig. S1).

That an accumulation of superoxide in the brain precedes the accumulation in the midgut (Fig. 1 *E* and *F*) raised the question of whether a ROS signal generated in the nervous system may spread to other tissues. Indeed, knockdown of a mitochondrial complex 1 subunit (*ND42*) as well as a mitofusin (*Marf*) in the brain caused an increase in the numbers of LDs in the fat body and reduction in the Malpighian tubules (Fig. 2 *A* and *B*).

Downloaded by guest on September 30, 2020

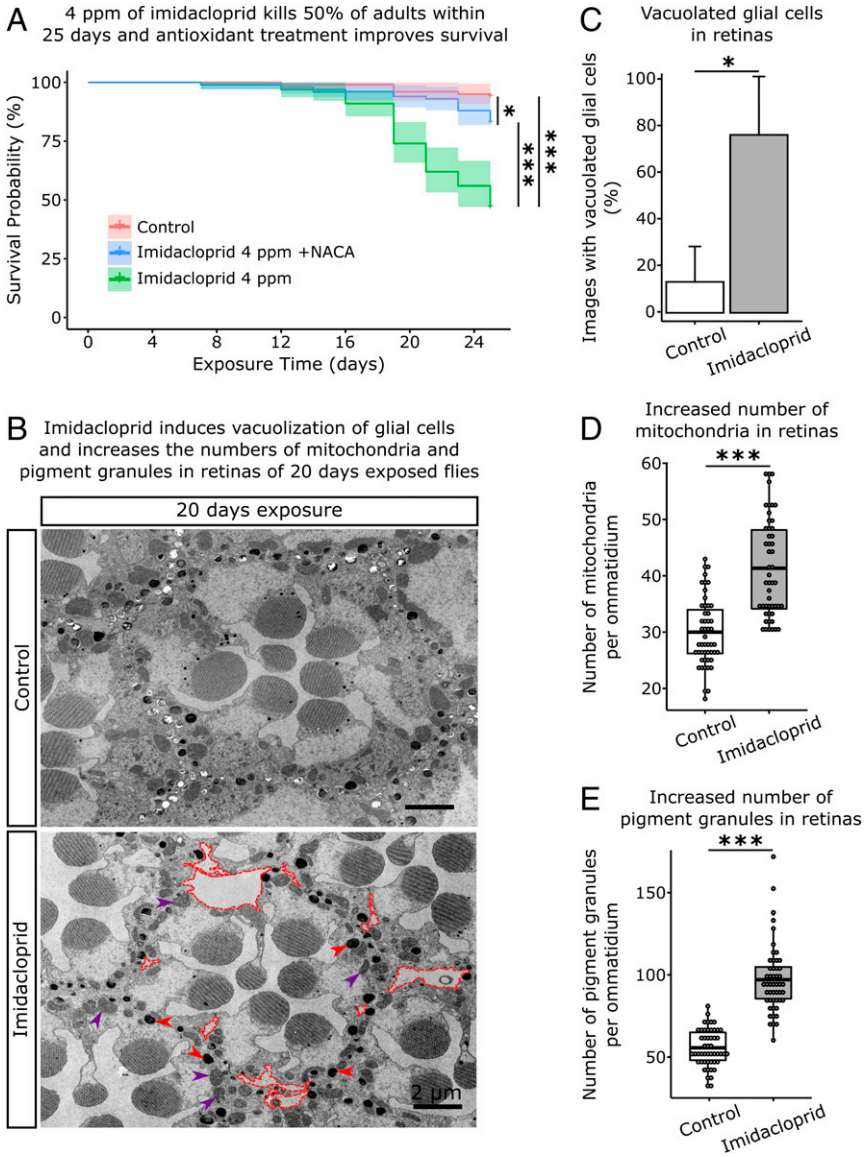

Fig. 6. Low dose chronic exposures reduce survival and cause degeneration in the retina. (*A*) Survival of adults continuously exposed to 4 ppm imidacloprid. A total of 47% of adults were alive after 25 d of exposure. Flies exposed to the same dose of imidacloprid in media supplemented with 75 μg/L of NACA show 83% survival. Significance assessed with the Kaplan–Meier method and the Log-rank Mantel–Cox test ($n = 100$ adult flies/treatment), $^*P < 0.05$; $^{***}P < 0.001$. (*B*) Electron microscopy of the retinas of flies exposed for 20 d. Dashed red lines delimitate vacuoles in glia, red arrowheads point to pigment granules, and purple arrowheads point to mitochondria. (Scale bar: 2 μm.) (*C*) Percentage of images that show vacuolated glial cells in the retina (10 images/adult fly; 3 adult flies/treatment). (*D*) Number of mitochondria per ommatidium (16 ommatidia/adult fly; 3 adult flies/treatment). (*E*) Number of pigment granules per ommatidium (16 ommatidia/adult fly; 3 adult flies/treatment). Shaded areas in *A* represent 95% confidence interval. *C*, *D*, and *E*, *t* test; $^*P < 0.05$; $^{***}P < 0.001$.

Exposure to imidacloprid precipitated similar LD phenotypes (Fig. 3 *A*–*D*). This was rescued by antioxidant pretreatment. ROS molecules are unstable and have a very short lifespan (53), which raises the question of how oxidative stress generated in the nervous system could spread to the fat body. More stable ROS, such as peroxidized lipids, are highly efficient in oxidizing other macromolecules (53). Considering the proximity of the larval brain and enteric neurons to fat body (54) it is possible that oxidizing agents, such as peroxidized lipids, are transported through the hemolymph to the fat body or other tissues. This may account for the LD phenotypes in fat body and increased superoxide levels in the anterior midgut. An increase in insecticide metabolism in anterior midgut could also account for the superoxide increase (55) and if a ROS signal emanated from the midgut, it could also contribute to increasing LD numbers in the fat body.

The larval brain and fat body are observed to be responding very differently to imidacloprid exposure at the 2-h time point (*SI Appendix*, Table S2). The major xenobiotic stress response pathways, Cnc and JNK, are up-regulated in the brain, but not in the fat body. This may be because at this time superoxide levels are elevated in the brain, but not in the fat body. Our data provide evidence that the fat body may be mounting a protective response to elevated levels of ROS via increased numbers of LDs and lipid mobilization. LDs have the capacity to harbor lipids, protecting them from peroxidation (28). Decreased numbers of LDs in the midgut and Malpighian tubules (Fig. 3 and *SI Appendix*, Fig. S3) and the fat body transcriptomic data (*SI Appendix*, Table S2) provide evidence of lipid mobilization. It is

Downloaded by guest on September 30, 2020

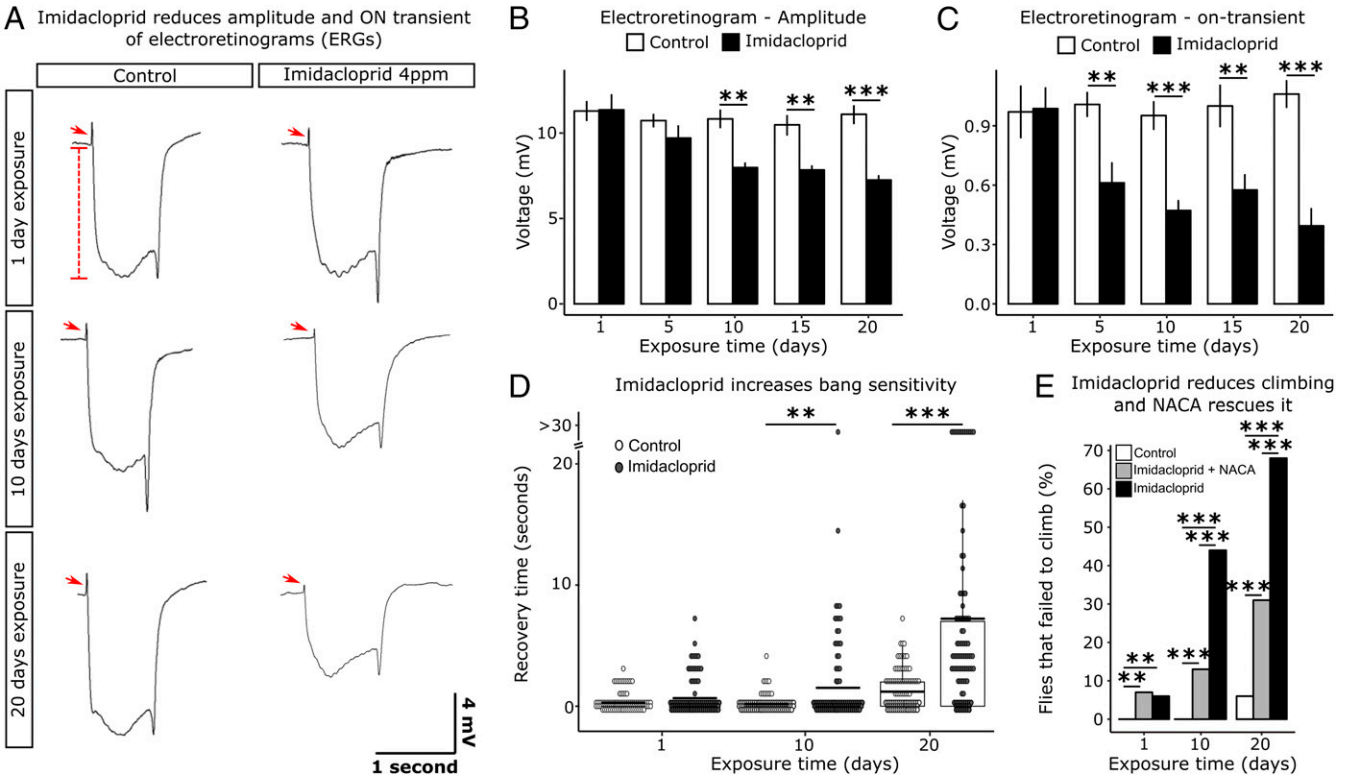

Fig. 7. Low dose chronic exposure reduces visual acuity and affects behavior. (*A*) Characterization of ERGs of animals exposed to imidacloprid for 1, 10, and 20 d. Red arrowheads indicate the on-transient signal and dashed red line the amplitude, both of which are reduced in exposed flies. (*B*) Amplitude of ERGs after 1, 5, 10, 15, and 20 d of exposure to imidacloprid ($n = 8$ to 10 adult flies/time point/treatment). (*C*) On-transient signal of ERGs after 1, 5, 10, 15, and 20 d of exposure to imidacloprid ($n = 8$ to 10 adult flies/time point/treatment). (*D*) Bang sensitivity of adults at 1, 10, and 20 d of exposure. Recovery time after 10 s vortexing at maximum speed was recorded in seconds for each fly ($n = 100$ adult flies/time point/treatment). (*E*) Percentage of adult flies that failed the climbing assay at 1, 10, and 20 d of exposure ($n = 100$ adult flies/time point/treatment). Flies exposed to the same doses of imidacloprid in media supplemented with 75 μg/L of NACA show a significant improvement in climbing ability after 10 and 20 d of exposure. Error bars in *B* and *C* represent mean ± SD *B* and *C*, *t* test; *D* and *E*, Wilcoxon test; $^{**}P < 0.01$; $^{***}P < 0.001$.

therefore possible that lipids are transported from the midgut and Malpighian tubules into the fat body. It is also possible that the Malpighian tubules excrete lipids. This has been shown to reduce the levels of peroxidized lipids under conditions of stress or injury (56). These hypotheses are not mutually exclusive.

The larval brain also differs in showing elevated expression of genes involved in the metabolism of lactate and pyruvate, suggesting an increased production of acetyl-CoA, building block for lipid synthesis (57). This, along with the accumulation of superoxide, creates the potential for the generation of peroxidized lipids (28). These processes were observed to occur in *Drosophila* adults linking ROS production, mitochondrial damage, and lipid peroxidation with neurodegeneration in the retina (26, 27). During a short-term low dose exposure the brain may be protected by the accumulation of these lipids into LDs, but ultimately such a defense may be overwhelmed, resulting in neurodegeneration (27). In this context, it is interesting to note that continuous exposure to an extremely low dose of imidacloprid (0.12 ppm) throughout larval life has been shown to lead to impacts on locomotor activity, sleep, and courtship and mating behavior in 3- to 7-d-old *Drosophila* adults (58). These aspects of behavior are also impacted in loss-of-function mutants for the nAChR α1 subunit targeted by imidacloprid (59, 60).

In adults, we find that defective mitochondria were present in photoreceptor cells in flies exposed to 4 ppm imidacloprid for 20 d. The observed vacuolization of glial cells is indicative of dying cells. Glial cells perform vital roles, providing support and protection for neurons and cleansing metabolites and toxic compounds generated by neuronal activity (61). The aberrant ERGs recorded for exposed flies demonstrate a loss of photoreceptor function and indicate that, under these conditions of exposure, imidacloprid causes blindness. While our analysis of the nervous system was limited to the visual system, the significant loss of climbing ability is indicative of neurodegeneration in other regions of the brain. That the loss of climbing ability was significantly rescued by NACA treatment indicates that oxidative stress contributes substantially to this behavioral defect. It is not clear which other regions of the brain are accessed by imidacloprid and/or the ROS signals that it triggers. The nAChR subunits targeted by imidacloprid are widely distributed in the brain (62). Hence, imidacloprid could impact a range of behaviors to which these subunits contribute. Observed changes in the levels of expression of several other receptor families noted in the transcriptome analysis could also drive behavioral changes. With a focus on the molecular mechanism by which imidacloprid acts, behavior has not been systematically examined here, but the analysis of a wider range of behavioral traits is warranted.

This study has focused on one widely used insecticide. It is likely that imidacloprid is not unique in its biological impact. Indeed, many other insecticides including organochlorines, organophosphates, carbamates, and pyrethroids may also induce oxidative stress (9–11, 14, 63). The targets of imidacloprid are conserved in insects (21), as are the pathways that generate oxidative stress in the nervous system in response to a sustained influx of calcium. Imidacloprid is therefore likely to cause oxidative stress in other species, triggering a similar cascade of downstream impacts. The concentrations at which this occurs

Downloaded by guest on September 30, 2020

will vary because there are marked differences in sensitivity to insecticides within and between species (42, 64). This is probably due to a wide range of factors, including those that influence the amount of insecticide reaching the brain such as insecticide metabolism, uptake, or efflux (65). For example, honey bees (*Apis mellifera*) are particularly sensitive to imidacloprid (66), which is known to cause oxidative stress in this species (14). Imidacloprid has been shown to target orthologous nAChR subunits in *A. mellifera* and *D. melanogaster*, but the *A. mellifera* receptors respond to an insecticide concentration an order of magnitude lower than the receptors of *D. melanogaster* (21). Further, *A. mellifera* has a reduced capacity to metabolize imidacloprid (66). The biomarkers identified here in the *Drosophila* system, such as ERGs, the anatomy of the retina, aconitase activity, ATP, and superoxide levels and LD dynamics could be used to investigate whether systemic impacts occur in other species at insecticide doses to which they may be exposed in the field.

There are widespread concerns about the contribution that insecticides, including imidacloprid, may be making insect populations decline. It is, therefore, worth considering how changes in insect biology observed here might impact nonpest insects in the field. If it occurred in other species, mitochondrial dysfunction leading to reduced ATP levels would impact energy-dependent processes ranging from vision (which uses 10% of all ATP daily), to reproductive output and the capacity to sustain flight. A shortening of lifespan would be critical in social insects such as honey bees, where workers take on different roles in the hive as they age. Impacts on the age structure of the hive, would impact the viability of the colony. Neurodegeneration could impact a range of behaviors, depending on the regions of the brain that are affected. The impairment of vision would constitute a threat to the survival of any insect. Defects in foraging behavior and visual learning have already been associated with imidacloprid exposure in honey bees (67). The significant down-regulation of genes involved in immune response identified here may compromise the capacity of insects to withstand biotic stresses. It has already been suggested that the humoral immune response of honey bees is compromised by insecticide exposure (68) and that it may be a factor in determining the extent of damage inflicted by the parasitic Varroa mite (69). Adaptation to any particular environment will rely on the regulation of gene expression to optimize phenotypic outcomes. The significant perturbations of gene expression observed here under conditions of acute exposure to low doses are very likely to disrupt fitness, particularly under conditions of stress. Consistent with this hypothesis, a tradeoff between the tolerance to imidacloprid and high temperatures has been reported for *Drosophila* (70).

The decline of insect populations around the world is a complex phenomenon with a variety of different factors suggested to be causal. It seems unlikely that any one factor will prove to be responsible and, indeed, different combinations of factors may explain declines in different parts of the world or for different species. The research here indicates a clear potential for insecticides to contribute and synergize with other stressors.

Materials and Methods

Detailed materials and methods are described in *SI Appendix*.

Fly Strains and Rearing. Armenia14 (line 14), an isofemale line derived from Armenia60 (*Drosophila* Genomics Resource Center #103394) (17), was used as the susceptible wild-type line for all assays except the following: For insecticide impact on mitochondrial turnover, the MitoTimer line (25) was used; for knockdown of mitochondrial genes in the central nervous system, UAS ND42 RNAi (Bloomington *Drosophila* Stock Center [BDSC] #28894) and UAS Marf RNAi (BDSC #55189) were crossed with Elav-Gal4 (BDSC #8760); as a control, UAS Luciferase RNAi (BDSC #31603) was crossed with Elav-Gal4 (BDSC #8760); and for the GCaMP experiment, UAS-tdTomato-P2A-GCaMP5G (III) (71, 72) was crossed with Dα6 T2A Gal4 (BDSC #76137). For experiments involving larvae, flies were reared on standard food media (*SI Appendix, Supplementary Material and Methods*) sprinkled with dried yeast and maintained at 25 °C. For experiments involving adults, flies were reared on molasses food (*SI Appendix, Supplementary Material and Methods*) and maintained at 25 °C. In all experiments involving adult flies, only females were used to maintain consistency.

Ca^{2+} Imaging in nAChR Expressing Neurons. Brains from Dα6 T2A Gal4 > UAS-tdTomato-2A-GCaMP5G third instar larvae were dissected and enzymatically digested in filtered HL-3 solution (70 mM NaCl, 5 mM KCl, 1 mM CaCl2, 20 mM MgCl2, 10 mM NaHCO3, 115 mM sucrose, 5 mM trehalose, and 5 mM Hepes) supplemented with 0.423 mM L-cysteine (Calbiochem) and 5 U/mL papain (Worthington). After 15 min, the brain tissues were washed twice with fresh Schneider's medium. The brain cells were dissociated by pipetting repeatedly. Cells were then plated on glass-bottom dishes (Corning) coated with Con A (C2010; Sigma-Aldrich). Cells were cultured in Schneider's medium supplemented with 10% fetal bovine serum, antibiotic-antimycotic (A5955; Sigma-Aldrich), and 50 μg/mL of insulin (I6634; Sigma-Aldrich) at room temperature. Cells were washed with phosphate-buffered saline (PBS) and replenished with fresh medium daily for 4 d before imaging experiments. Cytosolic [Ca^{2+}] imaging was performed using a Nikon A1 confocal microscope as described in ref. 73. Carbachol (100 μM) was used as a cholinergic agonist and thapsigargin (5 μM) as a SERCA inhibitor to release Ca^{2+} stores from the endoplasmic reticulum. Cytosolic Ca^{2+} levels were reported as GCaMP5G signal intensity divided by tdTomato signal intensity.

Evaluation of Lipid Environment of Metabolic Tissues in Larvae. Fat body, midgut, and Malpighian tubules were dissected in PBS (Ambion), fixed in 4% paraformaldehyde (PFA, Electron Microscopy Science), and subjected to lipid staining with Nile Red N3013 technical grade (Sigma-Aldrich). Images were obtained with a Leica SP5 laser scanning confocal microscope at 400× magnification.

Antioxidant Treatment. The antioxidant, NACA (AD4) was freshly prepared from powder before use by dissolving in distilled water. For acute exposures, larvae were pretreated with diluted NACA in 5% sucrose (Chem Supply) solution for 5 h prior to insecticide exposure assays. For chronic exposures, NACA was dissolved in the molasses food, cooked once a week, and replaced every second day.

Lipid Extraction and Analysis Using Liquid Chromatography-Mass Spectrometry. Lipidomic analyses of whole larvae exposed for 2 h to 2.5 ppm imidacloprid were performed in biological triplicate and analyzed by electrospray ionization-mass spectrometry (ESI-MS) using an Agilent Triple Quad 6410. Briefly, for lipid extraction, samples were transferred to CryoMill tubes and frozen in liquid nitrogen. A total of 200 μL of methanol containing 0.001% BHT (butylated hydroxytoluene, an organic lipophilic antioxidant) and 0.01 g/mL 13C5 valine (IS) were added to each CryoMill tube. Samples were subsequently homogenized (three × 45 s at 6,100 rpm, with 30-s rest between) using a CryoMill (Bertin Technologies) at −10 °C. Then 400 μL of chloroform was added to each tube and samples were incubated for 15 min at room temperature in a shaker at 1,200 rpm. Samples were then centrifuged for 15 min, at 13,000 rpm at room temperature; the supernatants were removed and transferred to new 1.5-mL microtubes. For a second wash, 100 μL of methanol (0.001% BHT and 0.01 g/mL 13C5 valine) and 200 μL of chloroform were added to CryoMill tubes, followed by vortexing and centrifugation as before. Supernatants were transferred to the previous 1.5-mL microtubes. A total of 300 μL of 0.1 M HCl was added to pooled supernatants and microtubes were then vortexed and centrifuged (15 min, room temperature, 13,000 rpm). Upper phases (lipid phases) were collected and transferred to clean 1.5-mL microtubes, as well as the lower phases (polar phases). All samples were kept at −20 °C until analysis. For liquid chromatography-mass spectrometry (LC-MS) analysis, microtubes were shaken for 30 min at 30 °C, then centrifuged at 100 rpm for 10 min at room temperature after which the supernatants were transferred to LC vials. Extracts were used for lipid analysis.

RNA Isolation and Transcriptomics Analysis (SRA Accession: PRJNA603631). Third instar larvae exposed to 2.5 ppm imidacloprid for 2 h were submitted to a tissue-specific transcriptomic analysis. Brains and fat bodies were dissected and independently used for RNA isolation. In total, three biological samples were prepared per tissue per treatment. Forty larvae were dissected for each biological sample. Samples were individually stored at −80 °C in 800 μL of TRIsure (Bioline). Total RNA was isolated following manufacturer's instructions. RNA purity and concentration were evaluated by spectrophotometry

Downloaded by guest on September 30, 2020

(NanoDrop ND-1000, NanoDrop Technologies) and RNA gel (1% agarose, 0.5% tris-borate-EDTA (TBE), run at 180 volts for 30 min). All samples had 2 μg of total RNA with an OD 260/280 ratio ≥1.9 and showed no signs of degradation. Samples were then diluted in 20 μL of nuclease-free water and transferred to GenTegra tubes, where RNA was further dried using SpeedVac. Dry RNA samples were shipped at ambient temperature to Novogene Co., Ltd for library preparation (NEBNext Ultra RNA Library Prep Kit), Illumina PE150 paired-end sequencing, and quantification analysis. The list of differentially expressed genes (DEGs) was used to perform Gene Ontology and KEGG pathway analysis using the software DAVID (Bioinformatics Resources 6.8). Only DEGs presenting foldchange > |2| and P adj < 0.05 were used for that purpose. The GO and KEGG terms generated were selected based on the criteria of presenting the modified Fisher exact P value <0.01.

Bang Sensitivity. The bang sensitivity phenotype was tested after 1, 10, and 20 d of chronic exposure to 4 ppm imidacloprid. Flies were vortexed on a VWR vortex at maximum strength for 10 s. The time required for flies to flip over and regain normal standing posture was then recorded.

Climbing Assay. Climbing phenotype was tested after 1, 10, and 20 d of exposure to 4 ppm imidacloprid. Five adult female flies were placed into a clean vial and allowed to rest for 30 min. Vials were tapped against a pad and the time required for the flies to climb up to a predetermined height (7 cm) was recorded. Flies that did not climb the predetermined height within 30 s were deemed to have failed the test.

Graphs and Statistical Analysis. All graphs were created, and all statistical analyses were performed in the software R (v.3.4.3). Images were designed using the free image software Inkscape (0.92.4).

Data Availability. The RNA-seq data generated in this study has been deposited with links to BioProject accession number PRJNA603631 in the National Center for Biotechnology Information (NCBI) BioProject database . All study data are included in the article and *SI Appendix*.

ACKNOWLEDGMENTS. F.M. was supported by a Victorian Latin America Doctoral Scholarship, an Alfred Nicholas Fellowship, and a University of Melbourne Faculty of Science Travelling Scholarship. P.B. was supported by The University of Melbourne. H.J.B. was supported by the Howard Hughes Medical Institute (HHMI) and is an investigator of HHMI. K.V. was supported by an NIH (National Institute on Aging) grant. Lipid analyses were performed at Metabolomics Australia at The University of Melbourne, which is a National Collaborative Research Infrastructure Strategy Initiative under Bioplatforms Australia Proprietary Ltd. (https://bioplatforms.com/).

1. N. E. Stork, How many species of insects and other terrestrial arthropods are there on earth? *Annu. Rev. Entomol.* **63**, 31–45 (2018).
2. P. Cardoso *et al*., Scientists' warning to humanity on insect extinctions. *Biol. Conserv.* **242**, 108426 (2020).
3. R. van Klink *et al*., Meta-analysis reveals declines in terrestrial but increases in freshwater insect abundances. *Science* **368**, 417–420 (2020).
4. F. Sánchez-Bayo, K. A. G. Wyckhuys, Worldwide decline of the entomofauna: A review of its drivers. *Biol. Conserv.* **232**, 8–27 (2019).
5. S. Cheng *et al*., Comparative susceptibility of thirteen selected pesticides to three different insect egg parasitoid Trichogramma species. *Ecotoxicol. Environ. Saf.* **166**, 86–91 (2018).
6. V. A. D'Ávila, W. F. Barbosa, R. N. C. Guedes, G. C. Cutler, Effects of spinosad, imidacloprid, and lambda-cyhalothrin on survival, parasitism, and reproduction of the aphid parasitoid aphidius colemani. *J. Econ. Entomol.* **111**, 1096–1103 (2018).
7. J. D. Crall *et al*., Neonicotinoid exposure disrupts bumblebee nest behavior, social networks, and thermoregulation. *Science* **362**, 683–686 (2018).
8. C. Mengoni Goñalons, W. M. Farina, Effects of sublethal doses of imidacloprid on young adult honeybee behaviour. *PLoS One* **10**, e0140814 (2015).
9. S. Karami-Mohajeri, M. Abdollahi, Toxic influence of organophosphate, carbamate, and organochlorine pesticides on cellular metabolism of lipids, proteins, and carbohydrates: A systematic review. *Hum. Exp. Toxicol.* **30**, 1119–1140 (2011).
10. A. Lukaszewicz-Hussain, Role of oxidative stress in organophosphate insecticide toxicity-Short review. *Pestic. Biochem. Physiol.* **98**, 145–150 (2010).
11. X. Wang *et al*., Permethrin-induced oxidative stress and toxicity and metabolism. A review. *Environ. Res.* **149**, 86–104 (2016).
12. T. Farooqui, A potential link among biogenic amines-based pesticides, learning and memory, and colony collapse disorder: A unique hypothesis. *Neurochem. Int.* **62**, 122–136 (2013).
13. J. Wu-Smart, M. Spivak, Sub-lethal effects of dietary neonicotinoid insecticide exposure on honey bee queen fecundity and colony development. *Sci. Rep.* **6**, 32108 (2016).
14. K. V. B. Balieira *et al*., Imidacloprid-induced oxidative stress in honey bees and the antioxidant action of caffeine. *Apidologie* **49**, 562–572 (2018).
15. T. C. Sparks, R. Nauen, IRAC: Mode of action classification and insecticide resistance management. *Pestic. Biochem. Physiol.* **121**, 122–128 (2015).
16. M. DiBartolomeis, S. Kegley, P. Mineau, R. Radford, K. Klein, An assessment of acute insecticide toxicity loading (AITL) of chemical pesticides used on agricultural land in the United States. *PLoS One* **14**, e0220029 (2019).
17. T. Perry, D. G. Heckel, J. A. McKenzie, P. Batterham, Mutations in Dalpha1 or Dbeta2 nicotinic acetylcholine receptor subunits can confer resistance to neonicotinoids in Drosophila melanogaster. *Insect Biochem. Mol. Biol.* **38**, 520–528 (2008).
18. H. Breer, D. B. Sattelle, Molecular properties and functions of insect acetylcholine receptors. *J. Insect Physiol.* **33**, 771–790 (1987).
19. S. Buckingham, B. Lapied, H. Corronc, F. Sattelle, Imidacloprid actions on insect neuronal acetylcholine receptors. *J. Exp. Biol.* **200**, 2685–2692 (1997).
20. P. Jeschke, R. Nauen, Neonicotinoids-from zero to hero in insecticide chemistry. *Pest Manag. Sci.* **64**, 1084–1098 (2008).
21. M. Ihara *et al*., Cofactor-enabled functional expression of fruit fly, honeybee, and bumblebee nicotinic receptors reveals picomolar neonicotinoid actions. *Proc. Natl. Acad. Sci. U.S.A.* **117**, 16283–16291 (2020).
22. Bayer Crop Science Australia (2019). Confidor® 200 SC Insecticide. Available at: https://www.crop.bayer.com.au/find-crop-solutions/by-product/insecticides/confidor-200-sc-insecticide. Accessed 15 October 2019.
23. P. S. Brookes, Y. Yoon, J. L. Robotham, M. W. Anders, S. S. Sheu, Calcium, ATP, and ROS: A mitochondrial love-hate triangle. *Am. J. Physiol. Cell Physiol.* **287**, C817–C833 (2004).
24. L. J. Yan, R. L. Levine, R. S. Sohal, Oxidative damage during aging targets mitochondrial aconitase. *Proc. Natl. Acad. Sci. U.S.A.* **94**, 11168–11172 (1997).
25. R. A. Gottlieb, A. Stotland, MitoTimer: A novel protein for monitoring mitochondrial turnover in the heart. *J. Mol. Med.* **93**, 271–278 (2015).
26. L. Liu *et al*., Glial lipid droplets and ROS induced by mitochondrial defects promote neurodegeneration. *Cell* **160**, 177–190 (2015).
27. L. Liu, K. Mackenzie, N. Putluri, H. J. Bellen, The glia-neuron lactate shuttle and elevated ROS promote lipid synthesis in neurons and lipid droplet accumulation in glia via APOE/D. *Cell Metab.* **26**, 719–737.e6 (2017).
28. A. P. Bailey *et al*., Antioxidant role for lipid droplets in a stem cell niche of *Drosophila*. *Cell* **163**, 340–353 (2015).
29. A. M. Schimel *et al*., N-acetylcysteine amide (NACA) prevents retinal degeneration by up-regulating reduced glutathione production and reversing lipid peroxidation. *Am. J. Pathol.* **178**, 2032–2043 (2011).
30. X. L. Guan *et al*., Biochemical membrane lipidomics during *Drosophila* development. *Dev. Cell* **24**, 98–111 (2013).
31. R. Dawaliby *et al*., Phosphatidylethanolamine is a key regulator of membrane fluidity in eukaryotic cells. *J. Biol. Chem.* **291**, 3658–3667 (2016).
32. N. Krahmer *et al*., Phosphatidylcholine synthesis for lipid droplet expansion is mediated by localized activation of CTP:phosphocholine cytidylyltransferase. *Cell Metab.* **14**, 504–515 (2011).
33. Z. Liu, X. Huang, Lipid metabolism in Drosophila: Development and disease. *Acta Biochim. Biophys. Sin.* **45**, 44–50 (2013).
34. M. Ren, C. K. L. Phoon, M. Schlame, Metabolism and function of mitochondrial cardiolipin. *Prog. Lipid Res.* **55**, 1–16 (2014).
35. A. Quintana, S. E. Kruse, R. P. Kapur, E. Sanz, R. D. Palmiter, Complex I deficiency due to loss of Ndufs4 in the brain results in progressive encephalopathy resembling Leigh syndrome. *Proc. Natl. Acad. Sci. U.S.A.* **107**, 10996–11001 (2010).
36. M. C. Wang *et al*., JNK signaling confers tolerance to oxidative stress and extends lifespan in *Drosophila*. *Dev. Cell* **5**, 811–816 (2003).
37. G. P. Sykiotis, D. Bohmann, Keap1/Nrf2 signaling regulates oxidative stress tolerance and lifespan in Drosophila. *Dev. Cell* **14**, 76–85 (2008).
38. J. R. Misra, G. Lam, C. S. Thummel, Constitutive activation of the Nrf2/Keap1 pathway in insecticide-resistant strains of Drosophila. *Insect Biochem. Mol. Biol.* **43**, 1116–1124 (2013).
39. A. Hahn, S. Zuryn, Mitochondrial genome (mtDNA) mutations that generate reactive oxygen species. *Antioxidants* **8**, 1–19 (2019).
40. G. Sirokmány, Á. Donkó, M. Geiszt, Nox/Duox family of NADPH oxidases: Lessons from knockout mouse models. *Trends Pharmacol. Sci.* **37**, 318–327 (2016).
41. H. Chung *et al*., Characterization of *Drosophila* melanogaster cytochrome P450 genes. *Proc. Natl. Acad. Sci. U.S.A.* **106**, 5731–5736 (2009).
42. S. Denecke *et al*., Multiple P450s and variation in neuronal genes underpins the response to the insecticide imidacloprid in a population of *Drosophila melanogaster*. *Sci. Rep.* **7**, 11338 (2017).
43. O. I. Azeez, R. Meintjes, J. P. Chamunorwa, Fat body, fat pad and adipose tissues in invertebrates and vertebrates: The nexus. *Lipids Health Dis.* **13**, 71 (2014).
44. A. Brandt, A. Gorenflo, R. Siede, M. Meixner, R. Büchler, The neonicotinoids thiacloprid, imidacloprid, and clothianidin affect the immunocompetence of honey bees (*Apis mellifera L.*). *J. Insect Physiol.* **86**, 40–47 (2016).
45. G. Di Prisco *et al*., Neonicotinoid clothianidin adversely affects insect immunity and promotes replication of a viral pathogen in honey bees. *Proc. Natl. Acad. Sci. U.S.A.* **110**, 18466–18471 (2013).
46. N. Buchon, N. Silverman, S. Cherry, Immunity in *Drosophila melanogaster*–from microbial recognition to whole-organism physiology. *Nat. Rev. Immunol.* **14**, 796–810 (2014).
47. H. J. Gao *et al*., Preventive effects of N-acetyl-l-cysteine against imidacloprid intoxication on *Bombyx mori* larvae. *Arch. Insect Biochem. Physiol.* **99**, e21497 (2018).
48. T. Wenz, Regulation of mitochondrial biogenesis and PGC-1α under cellular stress. *Mitochondrion* **13**, 134–142 (2013).

Downloaded by guest on September 30, 2020

49. J. E. Niven, J. C. Anderson, S. B. Laughlin, Fly photoreceptors demonstrate energy-information trade-offs in neural coding. *PLoS Biol.* **5**, e116 (2007).
50. T. Wang, C. Montell, Phototransduction and retinal degeneration in *Drosophila*. *Pflugers Arch.* **454**, 821–847 (2007).
51. P. Pavlidis, M. A. Tanouye, Seizures and failures in the giant fiber pathway of *Drosophila* bang-sensitive paralytic mutants. *J. Neurosci.* **15**, 5810–5819 (1995).
52. L. McGurk, A. Berson, N. M. Bonini, Drosophila as an in vivo model for human neurodegenerative disease. *Genetics* **201**, 377–402 (2015).
53. M. Valko *et al*., Free radicals and antioxidants in normal physiological functions and human disease. *Int. J. Biochem. Cell Biol.* **39**, 44–84 (2007).
54. D. Padmanabha, K. D. Baker, Drosophila gains traction as a repurposed tool to investigate metabolism. *Trends Endocrinol. Metab.* **25**, 518–527 (2014).
55. D. G. Deavall, E. A. Martin, J. M. Horner, R. Roberts, Drug-induced oxidative stress and toxicity. *J. Toxicol.* **2012**, 645460 (2012).
56. X. Li, S. Rommelaere, S. Kondo, B. Lemaitre, Renal purge of hemolymphatic lipids prevents the accumulation of ROS-induced inflammatory oxidized lipids and protects *Drosophila* from tissue damage. *Immunity* **52**, 374–387.e6 (2020).
57. N. C. Williams, L. A. J. O'Neill, A role for the krebs cycle intermediate citrate in metabolic reprogramming in innate immunity and inflammation. *Front. Immunol.* **9**, 141 (2018).
58. H. K. Young, S. M. Denecke, C. Robin, A. Fournier-Level, Sublethal larval exposure to imidacloprid impacts adult behaviour in Drosophila melanogaster. *J. Evol. Biol.* **33**, 151–164 (2020).
59. J. Somers, H. N. B. Luong, P. Batterham, T. Perry, Deletion of the nicotinic acetylcholine receptor subunit gene Dα1 confers insecticide resistance, but at what cost? *Fly* **12**, 46–54 (2018).
60. J. Somers, H. N. B. Luong, J. Mitchell, P. Batterham, T. Perry, Pleiotropic effects of loss of the Dα1 subunit in Drosophila melanogaster: Implications for insecticide resistance. *Genetics* **205**, 263–271 (2017).
61. M. R. Freeman, *Drosophila* central nervous system glia. *Cold Spring Harb. Perspect. Biol.* **7**, 1–14 (2015).
62. V. Croset, C. D. Treiber, S. Waddell, Cellular diversity in the *Drosophila* midbrain revealed by single-cell transcriptomics. *eLife* **7**, 1–31 (2018).
63. S. Terhzaz *et al*., A novel role of *Drosophila* cytochrome P450-4e3 in permethrin insecticide tolerance. *Insect Biochem. Mol. Biol.* **67**, 38–46 (2015).
64. C. Manjon *et al*., Unravelling the molecular determinants of bee sensitivity to neonicotinoid insecticides. *Curr. Biol.* **28**, 1137–1143.e5 (2018).
65. J. G. Scott, N. Buchon, *Drosophila melanogaster* as a powerful tool for studying insect toxicology. *Pestic. Biochem. Physiol.* **161**, 95–103 (2019).
66. T. Iwasa, N. Motoyama, J. T. Ambrose, R. M. Roe, Mechanism for the differential toxicity of neonicotinoid insecticides in the honey bee, Apis mellifera. *Crop Prot.* **23**, 371–378 (2004).
67. L. P. Belzunces, S. Tchamitchian, J. L. Brunet, Neural effects of insecticides in the honey bee. *Apidologie* **43**, 348–370 (2012).
68. N. Perveen, M. Ahmad, Toxicity of some insecticides to the haemocytes of giant honeybee, *Apis dorsata* F. under laboratory conditions. *Saudi J. Biol. Sci.* **24**, 1016–1022 (2017).
69. F. Nazzi, Y. Le Conte, Ecology of *Varroa destructor*, the Major Ectoparasite of the Western Honey Bee, Apis mellifera. *Annu. Rev. Entomol.* **61**, 417–432 (2016).
70. A. Fournier-Level *et al*., The spread of resistance to imidacloprid is restricted by thermotolerance in natural populations of Drosophila melanogaster. *Nat. Ecol. Evol.* **3**, 647–656 (2019).
71. R. W. Daniels, A. J. Rossano, G. T. Macleod, B. Ganetzky, Expression of multiple transgenes from a single construct using viral 2A peptides in *Drosophila*. *PLoS One* **9**, e100637 (2014).
72. C. O. Wong *et al*., A TRPV channel in Drosophila motor neurons regulates presynaptic resting Ca2+ levels, synapse growth, and synaptic transmission. *Neuron* **84**, 764–777 (2014).
73. C. O. Wong *et al*., Lysosomal degradation is required for sustained phagocytosis of bacteria by macrophages. *Cell Host Microbe* **21**, 719–730.e6 (2017).

Downloaded by guest on September 30, 2020